Web of Discoveries: Journal of Analysis and Inventions
webofjournals.com/index.php/3

SYNTHESIS OF SNO_2 METAL OXIDE FILMS AND THEIR SENSITIVITY TO VARIOUS GASES

Usarov Khamidillo Saydullo ugli
Associate Professor, Andijan Branch,
Kokand University, PhD in Technical Sciences
https://orcid.org: 0009-0007-5590-9755,
e-mail: fizxamidullo91@mail.ru

Abstract

In this study, a tin dioxide (SnO_2)-based metal oxide film was deposited on a silicon (Si) substrate using the spray–pyrolysis technique of the sol–gel method. The influence of isothermal annealing on the structural and electrical properties of the obtained films was investigated, demonstrating that this treatment enhances the operational stability of the sensor. For SnO_2 metal oxide materials, the most critical and informative parameter is electrical conductivity (or resistivity), as even small variations in the analyzed gas concentration cause significant changes in the film's electrical resistance. The results indicate that SnO_2-based gas sensors exhibit high sensitivity to gases such as hydrogen sulfide (H_2S), freons, ethanol vapors, chlorine vapors, and hydrogen (H_2). For these gases, the sensors' sensitivity, operating temperature, and electrical characteristics were determined, allowing an assessment of their potential practical applications. The findings demonstrate that SnO_2 metal oxide films are promising candidates as gas-sensing elements for environmental monitoring and industrial safety systems.

Keywords: SnO_2 metal oxide, sol–gel, film, sensor, ethanol, isopropyl alcohol.

Introduction

In recent years, interest in gas sensors based on metal oxide semiconductors has increased significantly. Among these materials, tin dioxide (SnO_2) stands out due to its high chemical stability, wide bandgap energy, and high sensitivity to various gases. SnO_2-based sensors are widely used in environmental monitoring, industrial safety, medical applications, and consumer electronics [1–2].

SnO_2 metal oxide films can be fabricated using various physical and chemical methods. The most commonly employed techniques include sol–gel processing, chemical vapor deposition (CVD), physical vapor deposition (PVD), sputtering, spin-coating, and spray–pyrolysis. Films obtained by these methods exhibit significant differences in thickness, grain size, and surface morphology. In particular, the sol–gel and spray–pyrolysis methods attract considerable attention in practical applications due to their low cost and technological simplicity. The microstructure and surface area of the films directly affect the adsorption of gas molecules, which in turn enhances the sensor's sensitivity [3–4].

SnO_2 is an n-type semiconductor, and its gas sensitivity is primarily explained by adsorption and desorption processes occurring at its surface. In air, oxygen molecules adsorb onto the SnO_2

surface, capturing free electrons and increasing the resistance near the surface. When reducing gases such as CO, H_2, CH_4, NH_3, and others are introduced, they react with the adsorbed oxygen ions, returning electrons to the semiconductor. This results in a decrease in the electrical resistance of the SnO_2 film. Conversely, oxidizing gases such as NO_2 and O_3 capture additional electrons, causing the resistance to increase.

Due to the high sensitivity of SnO_2 films' electrical conductivity to changes in the surrounding gas composition, the development of metal oxide-based gas sensors emerged as a research direction. The first metal oxide gas sensor was developed by Taguchi in Japan in 1964, and its industrial-scale production continues today under Figaro Ltd. (Japan). TGS (Taguchi Gas Sensor) series sensors, manufactured by Figaro Ltd., feature a plastic housing equipped with a protective mesh against explosions. The sensors have four output pins: two for the heater and the remaining two for monitoring the electrical resistance of the sensing element.

These TGS sensors are based on SnO_2 and are widely used for detecting flammable gases in the air (e.g., propane, butane, ethanol, hydrogen) as well as toxic gases such as carbon monoxide, ammonia, sulfur dioxide, and others. Since methane is the primary component of natural gas, gas sensors are recommended to be installed in the basements of buildings to detect gas leaks. According to Japanese safety regulations, the installation of sensors to monitor natural gas leaks is mandatory in the basements of buildings with high occupancy. Currently, millions of gas sensors operate continuously in safety systems in Tokyo alone.

Tin dioxide (SnO_2) crystallizes in a rutile-type tetragonal structure and is one of the most stable compounds in the Sn–O system. In its structure, Sn^{4+} cations are surrounded by oxygen atoms forming octahedra (SnO_6), while O^{2-} anions occupy the centers of O–Sn_3 triangles. The crystal structure can be visualized as chains of edge-sharing SnO_6 octahedra, where the chains are connected at the octahedral vertices. The tetragonal unit cell parameters of SnO_2 are: a = b = 4.7374 Å, c = 3.1864 Å [5].

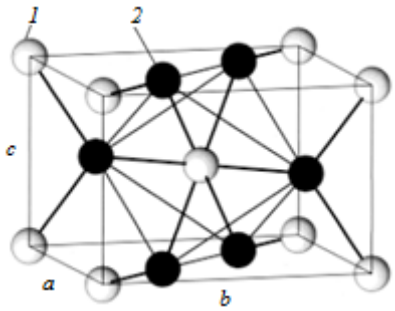

Figure 1. Crystal lattice of rutile-type tin dioxide (SnO_2) [5]: 1 – tin atom; 2 – oxygen atom; $a = b \neq c$

II. Physical Properties of Tin Dioxide (SnO_2) Metal Oxide Films

The physical properties of polycystalline metal oxide semiconductor films depend on their fabrication method, growth parameters, the presence of dopants, substrate material, and the type of gas environment. Additionally, post-deposition thermal treatments significantly influence the films' electrophysical properties. According to [6], thin SnO_2 films (~1.5 μm thick) prepared by spray deposition of $SnCl_4$ in ethanol exhibit a resistivity of approximately 154

Ω·cm in the undoped state and ~50 Ω·cm when doped with antimony, while the optical transmittance is ~68.2 %. SnO_2 layers are characterized by high optical transmittance, typically 80–90 %. As a substrate, K8 colorless optical glass provides over 90 % transparency. The light absorption ranges between 10–20 %, and the optical transmittance increases significantly as the film thickness decreases. For films with thicknesses of 0.07–0.09 μm, the average optical transmittance reaches 81–83 %. SnO_2 is transparent in the visible region and reflects infrared radiation with wavelengths greater than 2 μm. Based on the optical transmittance spectra, the absorption coefficient can be determined, allowing the evaluation of optical transitions, bandgap energy, and the film's stoichiometry.

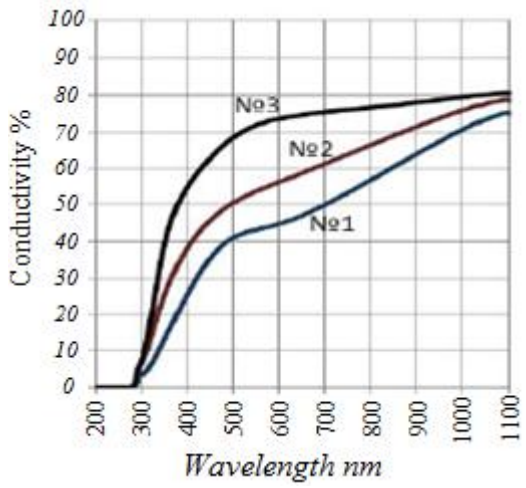

Figure 2. Optical transmittance spectra of SnO_2 samples №1, №2, and №3 after isothermal annealing at 300 °C for 1 hour.

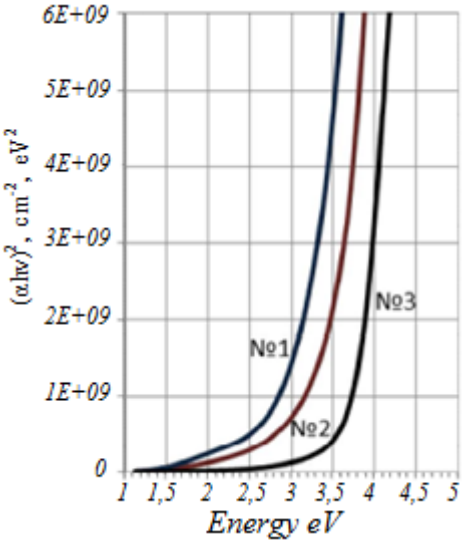

Figure 3. Dependence of (αhν)² on photon energy for SnO_2 samples №1, №2, and №3.

SnO_2 films were prepared using the sol–gel technique. To obtain the sol, 5 g of $SnCl_2 \cdot 2H_2O$ was dissolved in 25 ml of isopropyl alcohol (C_3H_8O) and stirred with a magnetic stirrer (IKA RH basic 2) at 100 °C for 20 minutes [7].

Using the sol–gel method, three SnO_2 film samples were prepared:

1. Sample №1 – after 8 hours, the solution remained in a sol state.
2. Sample №2 – after 10 hours, the solution began thickening.
3. Sample №3 – after 12 hours, the solution became a milky, viscous gel.

All samples were subsequently subjected to isothermal annealing at 300 °C for 1 hour. The optical transmittance spectra (Figure 2) indicate that Sample №3, prepared from the gel state, exhibits higher transparency compared to Samples №1 and №2, which had not yet fully gelled. The visible light transmittance of Sample №3 reaches 75 %.

Tin dioxide (SnO_2) is a direct-bandgap semiconductor. For direct allowed transitions, the absorption coefficient α is expressed as a function of photon energy , i.e., $\alpha=f(h\nu)$. In such cases, the plot of $(\alpha h\nu)^2$ versus is linear over a certain range. By extrapolating this linear region to intersect the abscissa, the bandgap energy (E_g) can be determined.

Figure 3 shows the dependence of on photon energy for SnO_2 samples №1, №2, and №3. Based on these data, the bandgap energies are as follows:

- Sample №1: $E_g \approx 3.0$ eV
- Sample №2: $E_g \approx 3.3$ eV
- Sample №3: $E_g \approx 3.7$ eV

The bandgap value of Sample №3 is closest to the true value of SnO_2 at room temperature. The lower E_g values for Samples №1 and №2 are attributed to oxygen non-stoichiometry arising during different stages of sol–gel film formation. Additionally, the electrical resistivity, carrier mobility, and free charge carrier concentration of the sol–gel-prepared SnO_2 films were measured, and the results are summarized in Table 1.

Table 1 Results of measurements of resistivity, carrier mobility, and free charge carrier concentration.

Sample number	R_s, kΩ	ρ, Ω·cm	μ, $cm^2/(V \cdot c)$	n, cm^{-3}
1	223,19	22,32	37,9	$7{,}39 \cdot 10^{15}$
2	294,32	29,43	61,69	$3{,}44 \cdot 10^{15}$
3	947,93	142,19	54,07	$8{,}13 \cdot 10^{14}$

Studies show that the electrical resistivity of SnO_2 samples synthesized before gelation (Samples №1 and №2) is relatively low, whereas the gel-based Sample №3, which exhibits the highest optical transparency, has a significantly higher resistivity. The surface electrical resistivity of SnO_2 films as a function of temperature was investigated, revealing that, regardless of the synthesis method, the resistivity is governed by two primary mechanisms (Figure 4) [8]:

1. First mechanism (150–200 °C): This regime is characteristic of semiconductors and is determined by the ionization of shallow donor states. As a result, the electrical resistivity decreases exponentially with increasing temperature.
2. Second mechanism (200–400 °C): In this range, the increase in resistivity is associated with oxygen vacancies in the film and the adsorption of oxygen from the atmosphere. The adsorbed oxygen captures electrons, leading to an increase in electrical resistivity.

SnO_2 is an n-type semiconductor with a wide bandgap, and its conductivity is mainly determined by oxygen vacancies in the crystal structure. These vacancies act as desorption centers for atmospheric oxygen. Depending on the temperature, the adsorbed oxygen on the SnO_2 surface can exist in different ionic forms — O_2^-, O^-, and O^{2-} — and the transitions between these forms are governed by specific temperatures and chemical reactions.

$$O_2(gaz) + e^{-1} \rightarrow O_2^-(adsor), \left(80 - 150\ ^0C\right)$$
$$O_2(adsor) + e^{-1} \rightarrow 2O^-(adsor), (150 - 260\ ^0C)$$
$$O\ (adsor) + e^{-1} \rightarrow O^{2-}(adsor), (300 - 500\ ^0C)$$

Adsorbed oxygen on the surface of tin dioxide (SnO_2) captures electrons from donor levels, leading to a reduction of electrons in the surface layer. As a result, the surface states become depleted, which causes an increase in the electrical resistivity of the films.

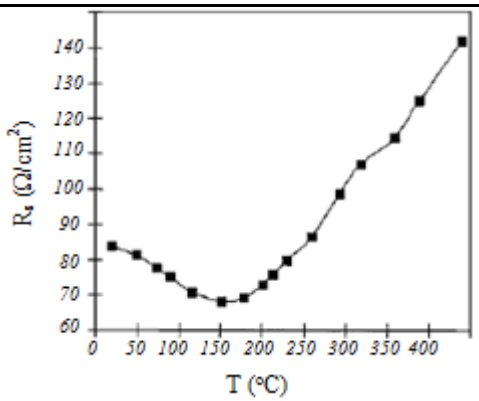

Figure 4. Temperature dependence of the surface electrical resistivity of tin dioxide (SnO_2) films.

Thus, the surface electrical resistivity of SnO_2 films is temperature-dependent and is governed by two competing processes:

In the range of 20–150 °C, the electrical conductivity is primarily determined by the ionization of donor states.

At temperatures above 150 °C, the dominant process is the desorption of oxygen, i.e., the adsorption of oxygen ions onto the film surface.

Within this temperature range, the distribution of charge carriers is largely influenced by the thermal vibrations of the crystal lattice.

III. Gas Sensitivity of SnO_2 Films

Currently, tin dioxide (SnO_2) is widely used in gas-sensitive semiconductor sensors. The operating principle of these sensors is based on changes in the physical parameters of the semiconductor material upon interaction with gas molecules. The physical parameters affected by gas adsorption on the semiconductor surface include electrical conductivity, work function, mobility of free charge carriers, surface charge carrier concentration, carrier lifetime, optical reflectance, and absorption coefficients. These parameters can be converted into the sensor's output signal, although not all are widely employed in practical applications.

For metal oxide semiconductors, particularly SnO_2, the most informative parameter is the electrical conductivity (or resistivity), because even small changes in gas concentration lead to significant variations in electrical resistivity (Figure 5).

Within the operating temperature range of 200–500 °C, the oxygen vacancies in SnO_2 films act as chemisorption centers for atmospheric oxygen. Adsorbed oxygen captures electrons from the donor levels, resulting in the formation of a Schottky potential barrier at the film surface. Meanwhile, the subsurface region of the film is enriched with a positively charged space-charge layer.

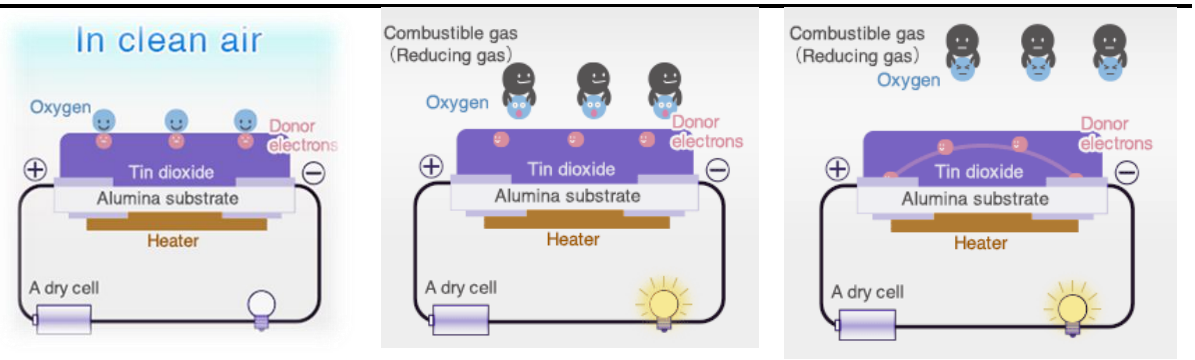

Figure 5. Operating mechanism of the SnO_2 gas sensor.

The electrical properties of tin dioxide (SnO_2) are influenced by chemisorption — that is, the chemical interaction of molecules with the material's surface — through two key parameters: the effective thickness of the surface layer and the height of the Schottky barrier. Depending on the structure of intergranular contacts in SnO_2, three types of electrical conduction mechanisms can be distinguished: bulk conduction, surface "barrier" conduction, and charge transport through Schottky barriers.

When analyzing the conduction mechanisms in polycrystalline SnO_2 films, several factors must be considered. Studies show that the gas sensitivity of metal oxide semiconductors strongly depends on the grain size and microstructure of the film. In polycrystalline films, a depleted surface layer devoid of electrons is formed, whose depth is determined by the Debye screening length (L_D) and the magnitude of the surface potential [9].

$$L_D = \left(\frac{\varepsilon_0 \varepsilon kT}{nq^2}\right)^{1/2}$$

The Debye length (L_D) is temperature-dependent. The thickness of the space-charge layer is typically related to the Debye length by the following ratio:

$$L = L_D \left(\frac{2eV_s}{kT}\right)^{1/2}$$

Here, V_S is the surface potential, and kT is the thermal energy. The approximation $L \approx 2L_D$ is valid only when $eV_S \ll kT$.

The polycrystalline metal oxide semiconductor film consists of grains of size D, which contact each other through grain boundaries, narrow channels, or primarily through narrow channels with partial boundary contact. Depending on the ratio between the grain size (D) and the thickness of the space-charge layer ($L \approx 2L_D$), three types of electrical conduction models and gas-sensing mechanisms can be distinguished:

1. Grain-boundary model ($D \gg 2L_D$): Characteristic of thick films with a high concentration of charge carriers. The film resistivity is primarily determined by the resistance at the grain-boundary contacts.
2. "Barrier" model ($D \geq 2L_D$): Characteristic of intermediate-thickness films. Conductivity occurs mainly through intergranular channels and partially via grain boundaries. The film resistivity is largely defined by the resistance of the channels.

3. Ultra-fine grain model ($D < 2L_D$): Characteristic of thin films. Electrical conduction occurs throughout the entire grains, and the film resistivity depends on the grain size.

The gas sensitivity of the films is defined as the ratio of the film resistance in air (R_v) to the resistance measured in a test gas at a known concentration (R_g):

$$S_g = \frac{R_v}{R_g}$$

Gas sensitivity is often expressed in terms of changes in electrical conductivity:

$$S'_g = \frac{G_g + G_v}{G_v} = \frac{G_g}{G_v} - 1$$

here

$$G_g = \frac{1}{R_g}$$

— The film's conductivity in the presence of the test gas,

$$G_v = \frac{1}{R_v}$$

— The film's conductivity in air.

Thus: $S'_g = \frac{R_v}{R_g} - 1 = S_g - 1$ [10]

The dependence of the gas sensitivity S'_g on the gas concentration represents the static gas-sensing characteristic of the SnO_2 film. The change of S_g over the contact time of the film with the gas environment defines its dynamic characteristic.

SnO_2-based gas sensors exhibit high sensitivity to hydrogen (H_2) in air, with a detection range of 0.001–2 vol.%. They can also detect hydrogen in a helium environment, with a range of 0.0001–2 vol.%.

Tin dioxide sensors are also capable of detecting the following gases:

- Hydrogen sulfide (H_2S): 0–300 mg/m³
- Freons: 0–10,000 mm/m³
- Ethanol vapors: 0–200 mg/m³
- Chlorine vapors: 0–200 mg/m³ [11]

Additionally, SnO_2-based sensors can be used for detecting carbon monoxide (CO). The measurable concentration range of CO is 500–3000 ppm.

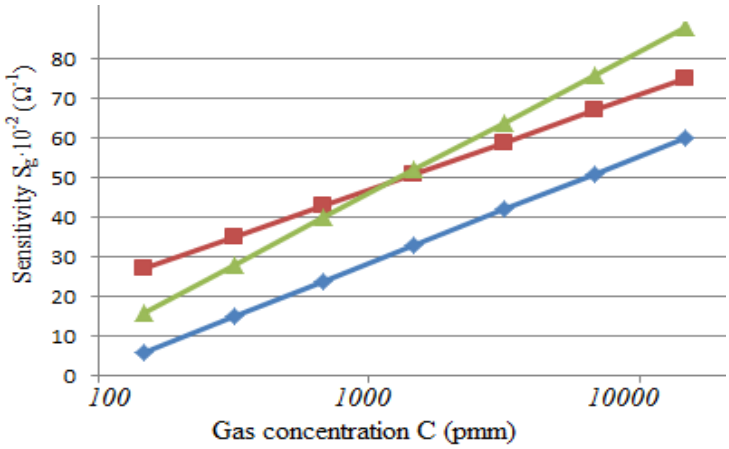

Figure 6. Dependence of the sensitivity of SnO_2 films on gas concentration.

The dynamic characteristics of gas sensitivity of SnO_2 films (Figure 6) allow determining the response time of the system when the gas environment changes. For acetone–air, ethanol–air, and propanol–air mixtures, this response time is approximately 5–10 minutes. After removing the test gas mixture, the film's resistance in air recovers within 2–3 minutes. The data indicate that the sensitivity increases with gas concentration, with the highest sensitivity observed in Sample 3, reflecting the film structure's high adaptability to surface reactions.

IV. Conclusion

Thus, the study demonstrates that isothermal treatment increases on the SnO_2 sensing layer and releases oxygen-containing chemical bonds, resulting in enhanced stability of the gas sensors and improved electronic transport properties of the film. Furthermore, doping the SnO_2 sensing layer with Ag improves the samples' metrological characteristics—including sensitivity, selectivity, and power consumption—making them suitable for the selective detection of toxic and explosive gases.

References

1. Rahul Kumar, Mamta, Raman Kumari, Vidya Nand Singh. SnO_2-Based NO_2 Gas Sensor with Outstanding Sensing Performance at Room Temperature. Micromachines. 2023, 14(4), 728; https://doi.org/10.3390/mi14040728.
2. Pengfei Liu, Jianbin Wang, Han Jin, Meiying Ge, Fang Zhang, Cheng Wang, Yan Sun, Ning Dai. SnO_2 mesoporous nanoparticle-based gas sensor for highly sensitive and low concentration formaldehyde detection. National Library of Medicine. 2023 Jan 13; 13(4): 2256–2264. https://doi.org/10.1039/d2ra06745e
3. Shrestha Tyagi, Manika Chaudhary, Anit K. Ambedkar, Kavita Sharma, Yogendra K. Gautam, Beer Pal Singh. Metal oxide nanomaterial-based sensors for monitoring environmental NO_2 and its impact on the plant ecosystem: a review. Royal Society of Chemistry. 2022, 106–129. https://doi.org/10.1039/d1sd00034a
4. Arunkumar Shanmugasundaram, Karthikeyan Munirathinam, Dong‑Weon Lee. SnO_2 nanostructure-based acetone sensors for breath analysis. Micro and Nano Systems Letters (2024) 12:3 https://doi.org/10.1186/s40486-023-00196-5.
5. Kovalenko, V. V. Surface chemistry of nanocrystalline SnO_2: effect of thermal treatment and additives / V. V. Kovalenko, A. A. Zhukova, M. N. Rumyantseva et. al. // Sensors and Actuators. – 2007. – V. 126.
6. Popova, L. I. Structure and morphology of thin SnO2 films / L. I. Popova, M .G. Michailov, V. K. Georguiev // Thin Solid Films. – 1990. – V. 186.
7. Onyiat, A. I. Fabrication and characterisation of tin oxide SnO_2 thin films using simple glass spray systems / A. I. Onyiat, C. B. Okeket // Journal of Applied Physics. – 1989. – V. 22.
8. Х.А. Махмудов, Ш.Х. Юлчиев, Ж.Н. Усмонов. Газочувствительные свойства пленок диоксида олова. Scientific bulletin. Physical and Mathematical Research. Vol. 4, Iss. 1. 2022.

9. Rembeza, S. I. Electrical resistivity and gas response mechanism of nanocrystalline SnO_2 films in a wide temperature range / S. I. Rembeza, E .S. Rembeza, T. V. Svistova et al. // Physica Status Solidi (A). – 2000. – V. 179.
10. Barsan, N. Conduction model in gas-sensing SnO_2 layers: grain-size effects and ambient atmosphere influence / N. Barsan //Sensor and Actuators. – 1994. – V. B. – № 17.
11. Watson, J. The tin dioxide gas sensor / J. Watson, K. Ihokura, G. S. V. Colest // Measurement Science and Technology. 1993. № 4.

Web of Discoveries: Journal of Analysis and Inventions
webofjournals.com/index.php/3